Correlation between Zirconium Tetra tert-Butoxide plasma phase and deposited layers

R. Verhoef[1], P. Raynaud[1], S. Ligot[2], R. Snyders[2,3], T. Nelis[4], R. Valledor Gonzalez[4], S. Vitale[4].

[1]*Université de Toulouse; UPS, CNRS; LAPLACE (Laboratory on Plasma and Conversion of Energy), 118 route de Narbonne, F-31062 Toulouse cedex 9, France.*
[2] *Chimie des Interaction Plasma surface, CIRMAP, UMONS – 23, place du Parc, B – 7000 Mons, Belgium.*
[3] *Materia NOVA Research Center – Parc Initialis, 1 Avenue Copernic, B – 7000 Mons, Belgium.*
[4] *Institute of Applied Laser, Photonics and Surface Technologies, ALPS. Bern University of Applied Sciences, Berner Fachhochschule (BFH), Quellgasse 21, CH-2501 Biel-Bienne, Switzerland*

Abstract: Leading to a better understanding of plasma deposition of Zirconium Tetra tert Butoxide (ZTB) experiments were carried out to describe the plasma decomposition process. $ZrO_xC_yH_z$ metal-organic thin films were deposited by low pressure RF coil inductive plasma, Fourier Transform Infrared Spectroscopy (FTIR) and Mass Spectrometry (MS) were used to investigate the gas and plasma phase.

Keywords: PECVD, ZTB, zirconium, decomposition, DFT, FTIR, MS, Plasma-surface.

1. Introduction

Plasma Enhanced Chemical Vapour Deposition (PECVD) using ZTB as precursor has been studied as way to deposit ZrO2. These coatings are promising due to their high dielectric constant (e, 14–25), wide band gap (Eg, 5.0–5.8 eV), high refractive index (n, 1.8–2.2), transparency, hardness, low thermal conductance, as well as oxidation resistance. These attributes make ZrO2 an excellent candidate for use in optical coatings (planar waveguides, broadband interference filters), microelectronics (gate dielectric in MOSFET), oxygen sensors, ionic conductors, and solid oxide fuel cell, as well as mechanically or thermally stable coatings (wear-resistance and thermal barrier coating). PECVD has a distinct advantage over conventional thermal CVD methods in that a higher deposition rate can be achieved at a much lower substrate temperature. Material and electrical characteristics of the deposited films depend on gas phase reactions because precursors are decomposed into highly reactive radicals by colliding with energetic plasma electrons in PECVD. Thus, to tune the properties of the deposited thin films a better understanding of the decomposition is essential. Here $ZrO_xC_yH_z$ metal-organic thin films were deposited by low pressure RF coil inductive plasma of pure zirconium Tetra tert-Butoxide (ZTB) as metal-organic precursor.

2. Experimental Setup

Zirconium Tetra tert Butoxide (Sigma-Aldricht, 99% purity) was plasma polymerized on Si wafers (110). The depositions were carried out in a metallic vacuum chamber 65 cm in length and 35 cm in diameter, pumped by a combination of turbomolecular and primary pumps allowing to reach a residual pressure lower than 2×10^{-6} Torr (**Error! Reference source not found.**). During the synthesis, the pressure varied from 2 to 4 mTorr. The plasma was generated using a one-turn inductive water-cooled copper coil (10 cm in diameter) located inside the chamber 10 cm in front of the substrate. The coil was connected to an Advanced Energy RF (13.56 MHz) power supply via a matching network. During the film depositions, substrate was at the floating potential, and the applied power (PRF) varied from 10 to 125 W. XPS measurements were performed using a PHI 5000 VersaProbe apparatus connected under vacuum to the

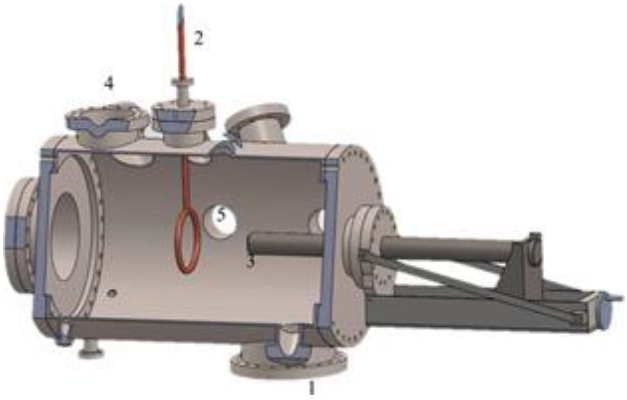

Fig. 1 3D experimental setup: 1, pumping system; 2, water-cooled RF copper coil; 3, substrate holder; 4, precursor inlet; 5, hidden

deposition chamber. Typically, the pressure in the analysis chamber was 5×10^{-9} Torr. A monochromatized Al Kα line (1486.6 eV) was used as a photon source. The plasma composition was investigated by a quadrupole HAL EQP 1000 mass spectrometer supplied by Hiden Analytical. The spectrometer was connected to the chamber by a 100µm extraction orifice. To allow detection of neutral species, they were ionized by electron impact (EI) with an electron kinetic energy fixed at 20eV in order to avoid excessive fragmentation of the precursor in the ionization chamber. DFT calculations were performed in order to optimize the geometries of the precursors and their fragments and to estimate the Gibbs free energy (at 298 K) of the associated reactions. For the calculations, the unrestricted B3LYP exchange-correlation functional with the 6-311++G(3df,3pd) basis set was employed. All calculations were performed using the Gaussian 09 package.

3. FTIR Results

Pure Zirconium Tetra tert Butoxide (ZTB) FTIR Spectra

The Beer Lambert law was checked at different pressures within the pressure range used in our experiments. Fig. **1** Pure ZTB FTIR spectrumFig. 1 shows a typical ZTB spectrum.

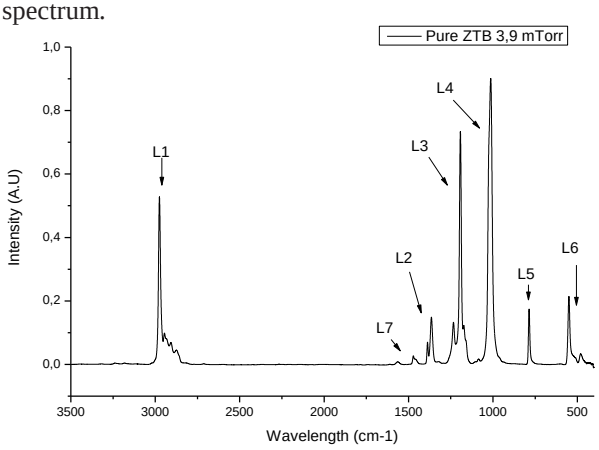

Fig. 1 Pure ZTB FTIR spectrum

Several identifications of ZTB bands have already been published [1,3,5], Table 1 lists the bands observed in the present study and their assignation.

This spectrum appears to be the spectrum of pure ZTB as it concurs with the theoretical spectrum calculated by DFT Fig. **2**.

Plasma ZTB versus Power

Fig. 3 shows FTIR spectra at different powers (0W, 45W and 125W). We can see that the spectral intensities are greatly reduced by the plasma state. At 45W the spectrum still contains many of the ZTB peaks while also presenting new peaks issued by the plasma decomposition. At higher power (125W) the ZTB peaks are really small. Table 2 shows the new peaks and their assignation by literature.

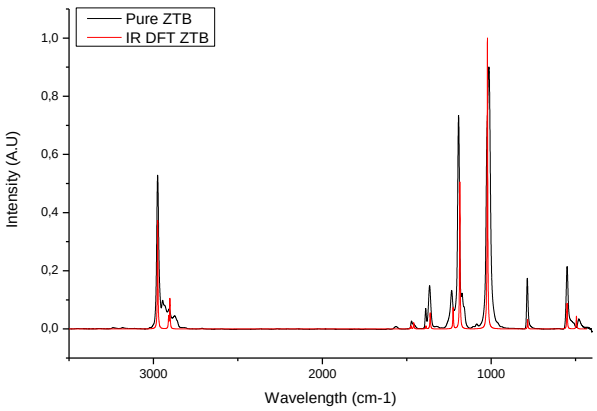

Fig. 2 DFT and FTIR of ZTB in gas phase

Table 1 Peaks of pure ZTB by FTIR

	Position (cm-1)	Vibration
L1	2975	νas CH3
	2946	νas CH3
	2934	νs CH3
	2907	νs CH3
	2875	νs CH2
	2861	νas CH3
L7	1564	νas CO
	1472	ρ + δs CH3
	1460	ρ + τ CH3
L2	1388	ω CH3
	1365	CH3
L3	1234	νas +δs C-CH3+ ν ZrO + ν CO
	1193	tert butyl stretching
	1173	ρ CH3
L4	1013	νs ZrO + δs C-CH3+ ν CO
L5	786	sym skeletal vibration of tert butyl group
L6	550	ZrO
	522	ZrO
	481	ZrO

4. MS results

Pure Zirconium Tetra tert Butoxide (ZTB) Mass Spectrum

Simultaneously to the FTIR measurements, Mass spectra were also acquired. The pure ZTB spectrum is to be found on Fig. 4. There is no evidence of mass 382, the mass of the complete ZTB molecule, only fragments can be found after ionisation. The Zr containing fragments could be easily identified in the mass spectrum using the relative abundance of naturally occurred Zr isotopes, i.e., ^{90}Zr (51%), ^{91}Zr (11%), ^{92}Zr (17%), ^{94}Zr (17%), and ^{96}Zr (3%). Other authors [2] already used this specific pattern to identify the presence of Zr in fragments. This way mass 367 is ZTB minus one CH3 group and 368 is ZTB minus CH3 plus H, showing evidence of hydrogen reattachment

inside the spectrometer. Table 3 list the principal identifications, most being accordance with Cho et al [2].

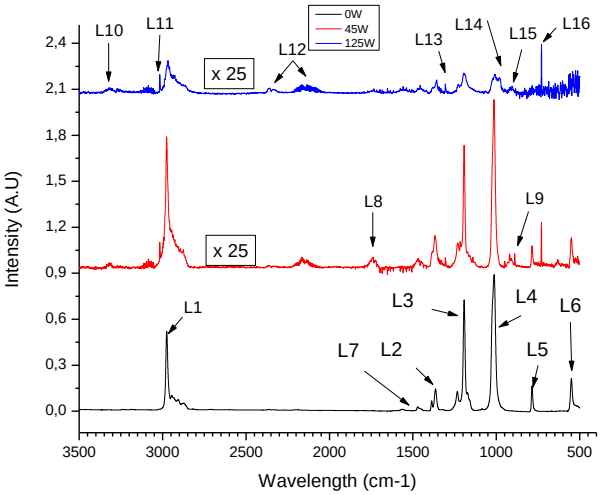

Fig. 3 FTIR spectra of pure ZTB and of plasma at 45W and at 125W

Table 2 Decomposition peaks for medium and high power

	Position (cm-1)	Assignation
L8	1747	
L9	889	
L10	3321	C2H4
L11	3016	CH4
L12	2359	CO
	2335	CO
	2148	CO2
L13	1305	CH4
L14	981	
L15	910	C2H2
L16	729	C2H4

Mass Spectra of ZTB plasma

The specta of ZTB plasma still show presence of the dissociation pattern of pure ZTB, namely 34% at 45W and 7% at 125W. Once the ZTB fragmentation pattern is subtracted the new peaks clearly stand out (Fig. 5, Fig. 6). The plasma peaks show a substantial increase in the H and H2 species and the 125W condition yields an intense H3 peak. The plasma spectra show no higher masses, sign of decomposition by the plasma. 125W plasma presents high count for low mass species and 45W shows higher counts for the intermediate masses (Fig. 5, Fig. 6). Mild power dissociates the mother molecule once, for example yielding OC(CH3)3 while higher power results in a dissociation of the daughter species, leaving only small fragments in the plasma.

Table 3 Mass assignations of ZTB gas and plasma phase

Mass	Name
1	H
2	H2
3	H3
13	CH
14	CH2
15	CH3
16	O + CH4
17	OH
18	H2O
19	H3O
26	C2H2
27	C2H3
28	C2H4 + CO
29	C2H5 + COH
30	C2H6 + OCH2
31	OCH3
32	O2
39	C2(CH3)
40	HC2(CH3)
41	2HC2(CH3)
42	C(CH3)2
43	OC(CH3)+ HC(CH3)2
44	CO2
45	(CH3)CH2 O
46	(CH3)CH2 OH
50	C4H2?
56	(CH2)C(CH3)2
72	C(CH3)4
91	ZrH
93	ZrH2
107	ZrOH
199	3(OH)ZrOC(CH3)2
255	ZTB - 2(OC(CH3)3) +H +OH
309	ZTB-OC(CH3)3
311	ZTB-OC(CH3)3 +2H
367	ZTB -CH3
368	ZTB -CH3 +H

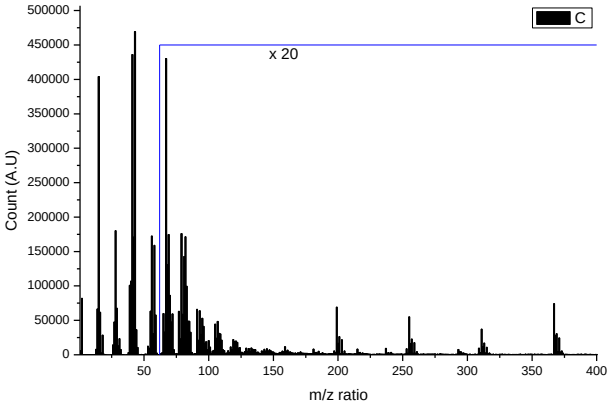

Fig. 4 Mass spectrum of pure ZTB

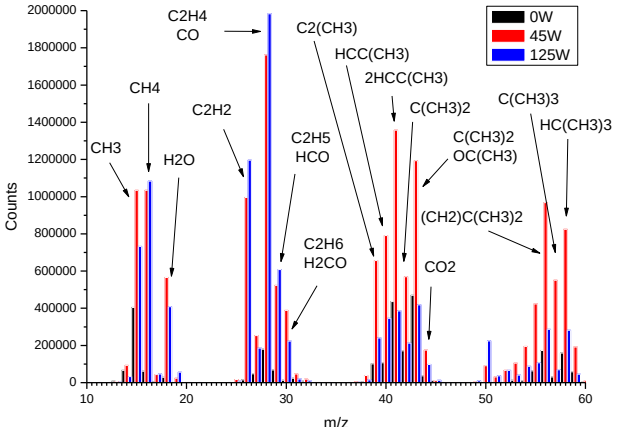

Fig. 5 Mass spectra of pure ZTB and 45W and 125W plasmas, m/z ranging from 10 to 60

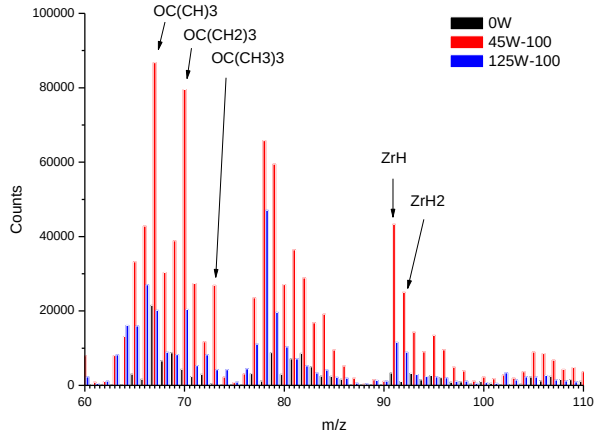

Fig. 6 Mass spectra of pure ZTB and 45W and 125W plasmas, m/z ranging from 60 to 110

5. Discussion

The accordance between the FTIR and the MS results shows coherence in the measurements but also in the assignations, be it by DFT calculations or literature. The decomposition of ZTB yields mainly classical fragments, CH4, C2H2, C2H4, CO and CO_2. The increase in plasma energy does increase the amount of precursor dissociated but also the extend of the dissociation. The low intensity of the FTIR signal for plasmas is explained by the fragmentation found by MS. The nature of the bonds stay identical but the amount of bonds is much lower. The fact that the parent molecule has 4 identical branches and yields fairly large fragments create the illusion of a parent molecule spectrum, while being in reality the addition of the fragments only the intensity signs for the decrease in bond density. The MS does not permit to discriminate between the CH4 and CO peak but the presence of low CO2 peaks in MS and small FTIR intensities for CO and CO2 rays indicates that the 28 peak contains mainly CH4. The equal count on C(CH3)3 and OC(CH3)3 coupled with the small amount of oxygen based species in FTIR and MS suggest half the bonds break before the oxygen and half after. This leaves a stripped core of ZrO2 fairly intense in FTIR but small in MS. The low count of ZrO2 by MS is probably due to the high sticking coefficient preventing the transport to the detector. XPS analysis of the deposited films show no marked difference in composition, only the deposition rate showed an increase with the applied power.

6. Acknowledgements

The author would like to thank R. Snyders to have granted access to the experimental setup at Materia Nova in MONS (Belgium). S.Ligot for having assisted the author to carry out the experiments. And finally M. Guillaume and the UMONS for carrying out the DFT calculations.

7. References

[1] M.A. Cameron and S.M. George. Zro2 film growth by chemical vapor deposition using zirconium tetra-tert-butoxide. *Thin Solid Films*, 348:90 – 98, 1999.

[2] Byeong-Ok Cho, Sandy X. Lao, and Jane P. Changa. Origin and effect of impurity incorporation in plasma-enhanced zro2 deposition. *Journal of Applied Physics*, 93(11):9345–9351, june 2003.

[3] Raphaël Cozzolino. *Etude de couches minces organométalliques déposées par procédé plasma basse pression à partir de Zirconium Tert Butoxide: application aux traitements antireflets*. PhD thesis, Université Toulouse III - Paul Sabastier, mars 2012.

[4] Laurent Denis, Philippe Marsal, Yoann Olivier, Thomas Godfroid, Roberto Lazzaroni, Michel Hecq, Jérome Cornil, and Rony Snyders. Deposition of functional organic thin films by pulsed plasma polymerization: A joint theoretical and experimental study. *Plasma Processes and Polymers*, 7(2):172–181, 2010.

[5] C. T. Lynch, K. S. Mazdiyasni, J. S. Smith and W. J. Crawford. Infrared spectra of transition metal alkoxides. *Analytical Chemistry*, 36(12):2332–2337, 1964.